Error-Disturbance Uncertainty Relations Simulated on a Quantum Computer

A.J. Rasmusson

A senior thesis submitted to the faculty of
Brigham Young University
in partial fulfillment of the requirements for the degree of

Bachelor of Science

Jean-François S. Van Huele, Advisor

Department of Physics and Astronomy

Brigham Young University

June 2018

ABSTRACT

Error-Disturbance Uncertainty Relations Simulated on a Quantum Computer

A.J. Rasmusson
Department of Physics and Astronomy, BYU
Bachelor of Science

Quantum measurement theory provides a relationship between measurement error and disturbance caused in observables due to measurement. This relationship describes the lower limit of error in quantum measurement. I expand current theory from two to three observables—two disturbances and one error—to better describe three dimensional properties (like spin). I create three quantum circuits, which together, represent error and two different disturbances in a spin-$\frac{1}{2}$ system. The quantum circuits are executed on IBM's real and simulated quantum computers. Simulated data match the two-observable relation while real data progressively gets further from the relation as the data approaches the relational boundary. For the two-observable relation, the quantum circuits are accurate on simulated quantum computers suggesting the inaccuracy in the real IBM quantum computers is due to internal IBM quantum computer workings. For three-observables, simulated and real quantum computer data suggest the constructed relation is not tight and thus not capturing the correct lower limit boundary. Tightening the three-observable relation is needed.

Keywords: [quantum measurement, error, disturbance error-disturbance uncertainty relation, quantum computing, quantum circuit, qubit model, quantum circuit, IBM Q Experience, Bloch Sphere]

Contents

Table of Contents **iii**

List of Figures **v**

1 Making Sense of Quantum Uncertainty **1**
1.1 Quantum Measurement Error and Disturbance 1
1.1.1 Definition of error 2
1.1.2 Definition of disturbance 3
1.2 Previous work by Ozawa and Branciard 3
1.2.1 Experimental verification 4
1.3 The IBM Q Experience 5
1.4 Motivation 7
1.5 Overview 9

2 Three-observable EDUR and Quantum Circuits **10**
2.1 Three-observable EDUR 10
2.1.1 Sum Method 11
2.1.2 Tightening the Three-observable EDUR 11
2.1.3 Application to Spin-$\frac{1}{2}$ Systems 12
2.2 Modeling EDURs with Qubits 13
2.2.1 Quantum Computing on the Bloch Sphere 13
2.2.2 Quantum Circuit of Error and Disturbance in EDURs 15

3 Results and Conclusion **19**
3.1 Verification of Two-observable EDUR in Application to Spin-$\frac{1}{2}$ 19
3.2 Verification of Three-observable EDUR in Application to Spin-$\frac{1}{2}$ 22
3.3 Conclusions 25
3.4 Future Work 25

Appendix A Quantum Computing Code **27**

Bibliography **33**

Index **36**

List of Figures

1.1 IBM Q Experience Composer Page 6

2.1 The Bloch Sphere 14

2.2 EDUR Quantum Circuit: Error in Y 17

2.3 EDUR Quantum Circuits: Disturbance in X and Z 18

3.1 Y Error and X Disturbance EDUR: Simulated (a) and Real (b) Quantum Computer Data 20

3.2 Y Error and Z Disturbance EDUR: Simulated (a) and Real (b) Quantum Computer Data 21

3.3 Three-observable EDUR: Simulated Quantum Computer Data 23

3.4 Three-observable EDUR: Real Quantum Computer Data 24

Chapter 1

Making Sense of Quantum Uncertainty

Quantum mechanics explains the foundations of our physical world. Yet, what explains the foundation of quantum mechanics? In this thesis, I explore, expand, and model quantum measurement by extending two-observable error-disturbance uncertainty relations (EDURs) to three observables and model two- and three-observable EDURs on IBM's quantum computers (both real and simulated devices).

1.1 Quantum Measurement Error and Disturbance

Contrasted to classical properties, quantum properties—observables—have a precision limit with which they can be measured. Consider a classical property, such as the mass of an object. In the classical physics view, the object's mass is definite and deterministic. Yet, a scale will display different mass values over repeated measurements. Classically speaking, this precision limitation is assumed to originate from the scale; an infinitely precise scale would read the same value every time.

Quantum mechanics tells a different story. In some cases, instead of the scale limiting the measurement precision, the actual observable is imprecise. This imprecision (and the resulting uncertainties) can be quantified and described by error-disturbance uncertainty relations (EDURs). Specifically, EDURs quantify the effect of successive measurements (e.g. measure A then B). The effect is quantified through error, disturbance, and standard deviation of the successive measurement observables and the observables' commutation. Because of the imprecision in the quantum world, EDURs are essential in tracking, predicting, and understanding why and how observables become (or are not) imprecise.

Under a different name, EDURs began with Heisenberg [1]. More recently Ozawa has modified and expanded EDURs [2–5]. Ozawa's work showed that by measuring two, disjoint observables, the measurement error of the first observable is linked to a disturbance of the second measured observable. In Sec. 1.1.1 and 1.1.2, I define error and disturbance according to Ozawa and briefly summarize the development of error-disturbance uncertainty relations since their original introduction in Sec. 1.2.

1.1.1 Definition of error

Conceptually, error is what you might expect: the difference between what you measure and the "true" value. Mathematically and quantum mechanically, Ozawa describes a quantum measurement's mean-square error as

$$\varepsilon(A)^2 = \mathrm{Tr}[(U^\dagger(\mathbb{1}\otimes M)U - A\otimes\mathbb{1})^2\rho\otimes|\xi\rangle\langle\xi|] \tag{1.1}$$

[2–5]. The measurement probe interaction U with the initial probe state $|\xi\rangle$ and a quantum state ρ describes the evolution of the measurement probe and the quantum state. Thus, the

difference between the probe observable M and the actual observable A of ρ is the error $\varepsilon(A)$ of the measurement [2–5].

1.1.2 Definition of disturbance

Quantum mechanical disturbance of an observable is caused by first measuring a non-commuting observable and then the observable that is ultimately disturbed. The more precise the first measurement of the non-commuting observable, the more disturbance in the second observable. Quantum mechanical disturbance, in the classical world, would be like measuring an objects length (one observable) and height. The more precisely you measurement the length, the more uncertain the height measurements come out. Though this never happens in the classical world, error and disturbance occur frequently in the quantum world. Ozawa describes the mean-square disturbance as

$$\eta(B)^2 = \mathrm{Tr}[(U^\dagger(B\otimes\mathbb{1})U - B\otimes\mathbb{1})^2\rho\otimes|\xi\rangle\langle\xi|] \tag{1.2}$$

[2–5]. The measurement probe interaction U and initial probe state $|\xi\rangle$ is the same as seen in the error definition Eq. (1.1). It is the interaction U of the probe $|\xi\rangle$ with the state ρ measuring A that disturbs the observable B. The difference between how B is affected by the probe—$U^\dagger(B\otimes\mathbb{1})U$—and B gives the mean-square disturbance of B [2–5].

1.2 Previous work by Ozawa and Branciard

The definitions of error and disturbance previously explained were first developed by Ozawa [2–5]. See also discussion in Ref. [6]. From these definition spring the current

EDURs. The current EDURs include an EDUR that is tighter for spin-$\frac{1}{2}$ that the general EDUR [7]. The tighter spin-$\frac{1}{2}$ were later extended to include mixed states [8]. I use the general EDUR and the tighter spin-$\frac{1}{2}$ specific EDUR including mixed states. The first EDUR has no state constricting assumptions for the spin-1/2 application, but it is not as tight for this spin-$\frac{1}{2}$ application [8]. The EDUR is

$$\varepsilon(A)^2\sigma(B)^2+\sigma(A)^2\eta(B)^2+2\varepsilon(A)\eta(B)\sqrt{\sigma(A)^2\sigma(B)^2-D_{AB}^2}\geq D_{AB}^2 \tag{1.3}$$

[8]. The tighter spin-$\frac{1}{2}$ specific EDUR includes constricting state assumptions. For this thesis, and spin-1/2 application, the relevant stricter assumptions are $\langle\psi|A|\psi\rangle=0$ and $\langle\psi|B|\psi\rangle=0$ [7,8]. The EDUR is

$$\hat{\varepsilon}(A)^2+\hat{\eta}(B)^2+2\hat{\varepsilon}(A)\hat{\eta}(B)\sqrt{1-D_{AB}^2}\geq D_{AB}^2 \tag{1.4}$$

where $\hat{\varepsilon}(A)=\varepsilon(A)\sqrt{1-\frac{\varepsilon(A)^2}{4}}$ and $\hat{\eta}(B)=\eta(B)\sqrt{1-\frac{\eta(B)^2}{4}}$ [7]. In both equations, D_{AB} is a commutator term $D_{AB}=\frac{1}{2}\mathrm{Tr}(\sqrt{\rho}[A,B]\sqrt{\rho})$ [8]. The $\sigma()^2$ terms are standard deviations (e.g. $\sigma(A)=\sqrt{\langle A^2\rangle-\langle A\rangle^2}$).

I will use both EDURs later on to form a three-observable EDUR. To verify and model the two- and three-observable EDURs, a scheme for measuring error and disturbance is needed.

1.2.1 Experimental verification

Ozawa proposed a way to measure error and disturbance called the three-state method [9, 10]. The three-state method finds the mean value of O_A and O_B—the observables as measured by an apparatus—in three different states to statistically find the error of the

actual observables A and B. The three-state method defines the square error and the square disturbance as

$$\varepsilon(A)^2 = 2 + \langle\psi| O_A |\psi\rangle + \langle A\psi| O_A |A\psi\rangle - \langle (A+\mathbb{1})\psi| O_A |(A+\mathbb{1})\psi\rangle \tag{1.5}$$

$$\eta(B)^2 = 2 + \langle\psi| O_B |\psi\rangle + \langle B\psi| O_B |B\psi\rangle - \langle (B+\mathbb{1})\psi| O_B |(B+\mathbb{1})\psi\rangle . \tag{1.6}$$

Both error and disturbance are made of three expectation values for three different states. The idea is that the first two expectation values measure any deviation from the desired measurement direction, while the third state measures along the measurement direction. Thus, the more deviation from the desired measurement axis (the first two expectation values) contributes to error while accurately measuring along the measurement direction (the last expectation value) takes away from the error.

Eqs. (1.5) and (1.6) make error and disturbance experimentally accessible. Experiments have successfully validated Ozawa's and Branciard's error-disturbance uncertainty relations in spin-$\frac{1}{2}$ systems, some using the three-state method [10–12]. In this thesis, I make quantum circuits from Eqs. (1.5) and (1.6) to model error and disturbance; those quantum circuits are then run on IBM's real and simulated quantum computers.

1.3 The IBM Q Experience

The IBM Q Experience is an open community with access to IBM's quantum computers. Currently, there are two 5-qubit and one 16-qubit quantum computers available [13]. Users have access to a full set of quantum gates providing users the full advantages of quantum computing [13].

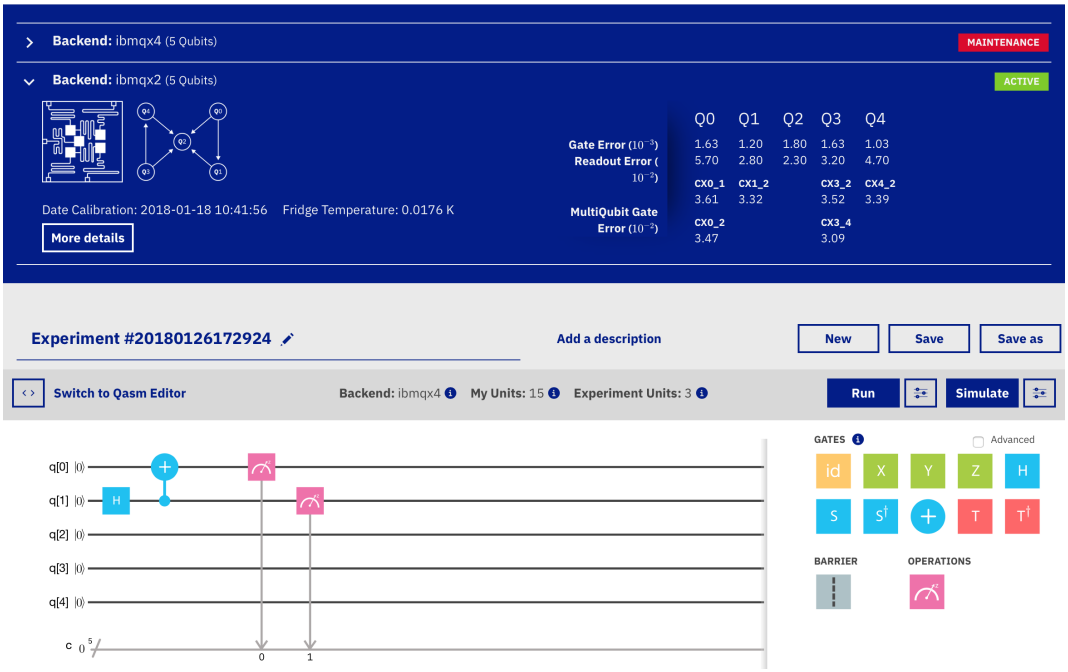

Figure 1.1 The IBM Q Experience composer page. In the top left are different quantum computers ("Backends") with calibration data to the right. The bottom half contains qubits represented by horizontal lines. The quantum gate selection on the right (colored boxes) can be applied to the qubits. In this case a Hadamard gate, controlled NOT gate and two measurement gates on qubits q[0] and q[1] are shown.

There are two ways of interfacing with IBM's quantum computers. Figure 1.1 shows the simplest way—the composer. The devices and calibration data are shown in the top blue region of Fig. 1.1. The selected device's qubits are shown in the bottom half labeled vertically "q[0], q[1], ... q[4]." The user can add gates to the qubits as shown with the blue and pink boxes on the qubits q[0] and q[1]. Gates lying on a qubit's line will be sequentially executed as a quantum circuit. All circuits must end with a measurement gate (seen in pink with the vertical line pointing down). The measurement gate maps the qubit to either a 0 for the ground state and 1 for the excited state.

The second way to interface with the quantum computers is through QISKit, the IBM Q Experience python package [14]. Though I did all my work in QISKit, the composer illustrates the process the qubits and gates best and will be used to show the completed error and disturbance quantum circuits.

1.4 Motivation

There is a gap in quantum uncertainty theory. To explain where this gap lies, I briefly review the development of quantum measurement theory.

Two kinds of quantum uncertainty exist. One is measurement uncertainty, described by error-disturbance uncertainty relations (EDURs). The other is the Heisenberg Uncertainty Principle [1], or Heisenberg Uncertainty relation (HUR). The HUR was later extended to any two non-commuting observables [15]. Three- (or even more) observable HURs have been derived, for example by Ma, et al. [16] and Quin et al. [17]. Ozawa and Branciard derived two-observable EDURs as discussed in Chapter 1. Table 1.1 organizes the developments by HUR or EDUR and two or three observables. The "missing" table entry in Table 1.1 is a main subject of this thesis.

Table 1.1 Quantum uncertainty relation table. Table of present theories classified by number of observables and type of quantum uncertainty. The "missing" table entry is the subject of my research.

	EDUR	HUR
2 Observables	Ozawa and Branciard [7, 8]	Heisenberg [1] and Robertson [15]
3 Observables	missing	Ma, et al. [16] and Qin et al. [17]

Though there are two-observable EDURs, a three-observable EDUR is needed. A three-observable EDUR captures the error and disturbances of physical systems which naturally occur in triplet (e.g. spin, position, and momentum have three observable components). Since many, if not most, physical systems have three components (e.g. x, y, and z components), theories describing measurement should naturally lend themselves to three observables. Analyzing the affect of measurement between the x and y components or x and z components is an incomplete picture. If we considered error along the x axis and disturbance along the y axis, we are leaving out information about the disturbance on z. There is no reason to believe a measurement of the spin in x would disturbance only y or only z. A three-observable EDUR's inclusion of the third component facilitates a complete picture of error and resulting disturbances.

The other focus of my thesis is the quantum circuitry for two- and three-observable. To validate the two-observable EDUR, previous experiments used neutron-optics or single photons [10–12]. However, studying quantum phenomena like measurement need not be restricted to expensive or complex laboratory setups. Using quantum computers, I modeled quantum measurement from my laptop. Modeling a quantum system on a quantum computer is different than traditional computational modeling. The qubits have quantum behavior analogous to the actual quantum particles; classical bits do not act like the physical system they model. Using this enhanced modeling from qubits (quantum modeling), two- and three-observable EDURs become simple to model with quantum circuits.

1.5 Overview

The goals of this thesis are to form a new three-observable EDUR (Sec. 2.1), and validate two- and three-observable EDURs through quantum circuits (Sec. 2.3) run on IBM's quantum computers (Sec. 3.1 and 3.2). In Sec. 2.1, I sum two two-observable EDURs to form a three-observable EDUR. This method accounts for the specific assumptions of two-observable EDURs and is a possible three-observable EDUR. In Sec. 2.3, I construct quantum circuits of one error and two disturbances based on the matrix form of the EDURs. In Sec. 3.1, I discuss the data results for the two-observable EDURs. In Sec. 3.2, the data from the two-observable EDUR is put together with the second disturbance creating the three-observable EDUR data set. Lastly, I discuss the data results for the three-observable EDUR.

Chapter 2

Three-observable EDUR and Quantum Circuits

In this chapter, I detail the expansion from two- to three-observable EDURs—motivated by the current lack of a three-observable EDUR (Table 1.1). After which, I detail the creation of quantum circuits for two- and three-observable EDURs applied to a spin-$\frac{1}{2}$ system. The data produced by the real and simulated quantum computers is used to evaluate both the two- and three-observable EDURs.

2.1 Three-observable EDUR

The ideal three-observable EDUR describes the error from a single measurement and the resulting disturbances in two other observables for a single state. The EDUR is constructed in two steps. First, in Sec. 2.1.1, summing two two-observable EDURs forms a three-observable EDUR. Second, in Sec. 2.1.2, the three-observable EDUR is tightened.

2.1.1 Sum Method

Summing two, two-observable EDURs with same error term, but different disturbances terms, gives a three-observable EDUR between three observables and describing one measurement interaction on one state. Thus, summing Eq. (1.3) with itself, after replacing the arbitrary B with an arbitrary C in the second equation, gives a general three-observable EDUR equation:

$$\begin{aligned} &\varepsilon(A)^2\sigma(B)^2+\sigma(A)^2\eta(B)^2+2\varepsilon(A)\eta(B)\sqrt{\sigma(A)^2\sigma(B)^2-D_{AB}^2} \\ &+\varepsilon(A)^2\sigma(C)^2+\sigma(A)^2\eta(C)^2+2\varepsilon(A)\eta(C)\sqrt{\sigma(A)^2\sigma(C)^2-D_{AC}^2} \\ &\geq D_{AB}^2+D_{AC}^2. \end{aligned} \tag{2.1}$$

Though this general form is universally valid, it can be tighter in the case of spin-$\frac{1}{2}$.

2.1.2 Tightening the Three-observable EDUR

The tightness of an inequality describes how close the bound is to the less than (or greater than) bound. The tighter an EDUR, the closer it is to describing the physical limiting precision inherent in quantum measurement. Thus, a tighter version of Eq. (2.1) is more descriptive and insightful. The sum of the two-observable EDURs cannot be any tighter than the original two observation equations, so I incorporate different two-observable EDURs to tighten the three-observable EDUR.

As mentioned in Sec. 1.2, Eq. (1.4) is tighter than Eq. (1.3). To construct a tighter three-observable EDUR, I sum Eq. (1.3), for observables A and B, with (1.4), for observ-

ables A and C. The result is a tighter three-observable EDUR:

$$\begin{aligned}\varepsilon(A)^2\sigma(B)^2+\sigma(A)^2\eta(B)^2+2\varepsilon(A)\eta(B)\sqrt{\sigma(A)^2\sigma(B)^2-D_{AB}^2}\\ +\hat{\varepsilon}(A)^2+\hat{\eta}(C)^2+2\hat{\varepsilon}(A)\hat{\eta}(C)\sqrt{1-D_{AC}^2}\\ \geq D_{AB}^2+D_{AC}^2\end{aligned} \tag{2.2}$$

where, again, $\hat{\varepsilon}(A)=\varepsilon(A)\sqrt{1-\frac{\varepsilon(A)^2}{4}}$ and $\hat{\eta}(C)=\eta(C)\sqrt{1-\frac{\eta(C)^2}{4}}$.

One may considered only using the tighter two-observable EDUR [Eq. (1.4)] in constructing the three-observable EDUR. However, summing the tighter EDUR equation with itself (in a similar manner) is not profitable. Under the assumptions of the tighter EDUR [Eq. (1.4)] $\langle\psi|A|\psi\rangle=\langle\psi|C|\psi\rangle=0$. If a second equation evaluated at A and B were added, $\langle\psi|A|\psi\rangle=\langle\psi|B|\psi\rangle=0$ must also be true for the system. Since I later apply the three-observable EDUR to spin-$\frac{1}{2}$, I know there is only *one* physical state ψ that meets both sets of assumptions—a totally mixed state. To include more states—but sacrifice some tightness—only one of the two two-observable EDURs in Eq. (2.2) can come from the tighter EDUR [Eq. (1.4)]; the other one must come from the more general EDUR [Eq. (1.3)]. As currently derived, states in Eq. (2.2) must satisfy $\langle\psi|A|\psi\rangle=\langle\psi|C|\psi\rangle=0$.

2.1.3 Application to Spin-$\frac{1}{2}$ Systems

In application to spin-$\frac{1}{2}$ systems, the tighter three-observable EDUR [Eq. (2.2)] can be simplified. Let $|\psi\rangle=\begin{bmatrix}1\\0\end{bmatrix}$., with the Pauli matrices $A=Y$, $B=Z$, and $C=X$, where

$$X=\begin{bmatrix}0&1\\1&0\end{bmatrix}\quad Y=\begin{bmatrix}0&-i\\i&0\end{bmatrix}\quad Z=\begin{bmatrix}1&0\\0&-1\end{bmatrix}. \tag{2.3}$$

The three-observable EDUR [Eq. (2.2)] neatly simplifies to

$$\hat{\eta}(X)^2 + \hat{\varepsilon}(Y)^2 + \eta(Z)^2 \geq 1, \tag{2.4}$$

where again $\hat{\varepsilon}(Y) = \varepsilon(Y)\sqrt{1-\frac{\varepsilon(Y)^2}{4}}$, $\hat{\eta}(X) = \eta(X)\sqrt{1-\frac{\eta(X)^2}{4}}$. Using two two-observable EDURs, I created a three-observable EDUR.

2.2 Modeling EDURs with Qubits

Qubits and quantum computing gates can represent physical quantum systems. Using quantum computers to model quantum measurement requires a "translation" from quantum mechanical operators and states to quantum computing gates and qubits. I refer to this as quantum circuitry or a quantum circuit. This is easily done using the matrix form of quantum operators, states, gates, qubits, and visualizing qubits on the Bloch sphere.

2.2.1 Quantum Computing on the Bloch Sphere

The quantum computer's qubits are best understood using the Bloch sphere (see Fig. 2.1) [13]. On the Bloch sphere, the vector pointing from the center to the edge of the sphere is a qubit (in red). Quantum gates rotate the vector. This simple model turns spin-$\frac{1}{2}$ quantum mechanics into simple rotations and vector projections that are easy to visualize and understand. The Bloch sphere helps define operators and prepare the correct qubits states.

Since the quantum circuits created were made for readable and not optimized or reduced to their simplest configuration, the circuits used the gates H, S, Y, Z, and $U3$. The

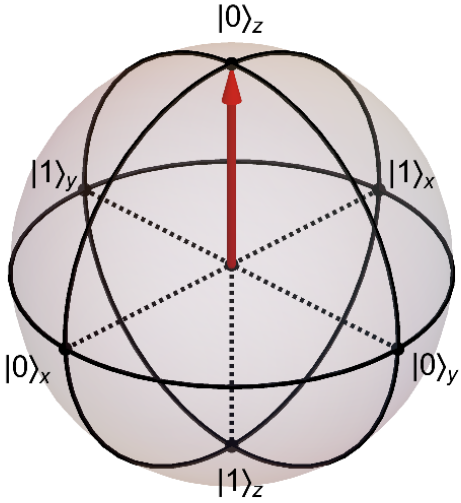

Figure 2.1 The Bloch sphere is a unit sphere often used to visualize what state a qubit is in and how quantum gates affect a qubit. The vector pointing from the center to the surface of the sphere represents the qubit. Quantum gates rotate the qubit: making the affects of quantum gates clear. The Bloch sphere captures the important imaginary and phase components of the qubit—completely describing it.

gates have the following standard matrix representations: $H = \frac{1}{\sqrt{2}}\begin{bmatrix} 1 & 1 \\ 1 & -1 \end{bmatrix}$, $S = \begin{bmatrix} 1 & 0 \\ 0 & i \end{bmatrix}$, $Y = \begin{bmatrix} 0 & -i \\ i & 0 \end{bmatrix}$, $Z = \begin{bmatrix} 1 & 0 \\ 0 & -1 \end{bmatrix}$, and $U3 = \begin{bmatrix} \cos\frac{\theta}{2} & -e^{i\lambda}\sin\frac{\theta}{2} \\ e^{i\phi}\sin\frac{\theta}{2} & e^{i\lambda+i\phi}\cos\frac{\theta}{2} \end{bmatrix}$. Each gate rotates the qubit in a different way. I will illustrate with a few examples. The Hadamard gate H rotates the qubit down from $|0\rangle_z$ to the $|0\rangle_x$, creating a superposition in the z basis. The S gate rotates the qubit $|0\rangle_x$ to $|0\rangle_y$. The Y gate rotates $|0\rangle_z$ to $|1\rangle_z$. The Z gate rotates $|0\rangle_x$ to $|1\rangle_x$. The $U3$ gate is the most general gate. It rotates the qubit by a polar angle θ and azimuthal angles ϕ and λ. This understanding of the gates is adequate for this thesis.

2.2.2 Quantum Circuit of Error and Disturbance in EDURs

Finding the right quantum gates and qubits to represent and model a quantum equation is best done in matrix form. This is because quantum gates and qubits are easily represented in matrix form. To translate from quantum equation to a series of qubits and quantum gates, quantum gates and qubits are matched to the matrix form of the quantum equation. There are two stages to matching. First, reconstruct initial quantum states from qubits and quantum gates. Second, reconstruct the main operator in the quantum equation from quantum gates. Staging the quantum circuit in this way makes the code more readable: The first stage prepares the qubit. The second stage operates on the qubit. (The qubits are then measured.)

Ozawa's three-state method for statistically measuring error [see Eqs. (1.5) and (1.6)] in matrix form is shown in Eq. (2.6). I want to explore all possible error and disturbance values, so O_A must be a matrix that can point to anywhere on the Bloch sphere given two angles, θ and ϕ (see Fig. 2.1) thus I choose

$$O_A = \begin{bmatrix} \cos\frac{\theta}{2} & e^{-i\phi}\sin\frac{\theta}{2} \\ e^{i\phi}\sin\frac{\theta}{2} & -\cos\frac{\theta}{2} \end{bmatrix}. \tag{2.5}$$

Evaluated for spin-$\frac{1}{2}$ where $|\psi\rangle = \begin{bmatrix} 1 \\ 0 \end{bmatrix}$ and $A = Y$, equation (1.5) now becomes

$$\varepsilon(Y)^2 = 2 + \begin{bmatrix} 1 & 0 \end{bmatrix} \cdot \begin{bmatrix} \cos\frac{\theta}{2} & e^{-i\phi}\sin\frac{\theta}{2} \\ e^{i\phi}\sin\frac{\theta}{2} & -\cos\frac{\theta}{2} \end{bmatrix} \cdot \begin{bmatrix} 1 \\ 0 \end{bmatrix} + \begin{bmatrix} 0 & -i \end{bmatrix} \cdot \begin{bmatrix} \cos\frac{\theta}{2} & e^{-i\phi}\sin\frac{\theta}{2} \\ e^{i\phi}\sin\frac{\theta}{2} & -\cos\frac{\theta}{2} \end{bmatrix} \cdot \begin{bmatrix} 0 \\ i \end{bmatrix} - \begin{bmatrix} 1 & -i \end{bmatrix} \cdot \begin{bmatrix} \cos\frac{\theta}{2} & e^{-i\phi}\sin\frac{\theta}{2} \\ e^{i\phi}\sin\frac{\theta}{2} & -\cos\frac{\theta}{2} \end{bmatrix} \cdot \begin{bmatrix} 1 \\ i \end{bmatrix} \tag{2.6}$$

and evaluates to

$$\varepsilon(Y)^2 = 2 - 2\sin(\frac{\theta}{2})\sin(\phi). \tag{2.7}$$

Each expectation value [three in Eq. (2.6)] is assigned to one qubit.

The matrix representation of qubit states on the Bloch sphere (shown in Fig. 2.1) makes it easy to identify what gates are needed to correctly construct the qubits. All qubits initialize in the state $\begin{bmatrix} 1 \\ 0 \end{bmatrix}$. The state for the first expectation value is already in the initialized qubit state, so no state preparation is needed. To reconstruct the state for the second expectation value, I apply a Y gate to ψ, $Y\psi = \begin{bmatrix} 0 \\ i \end{bmatrix}$. The state for the third expectation value is constructed as $SH\psi = \frac{1}{\sqrt{2}} \begin{bmatrix} 1 \\ i \end{bmatrix}$. The expectation value of the third qubit is smaller by a factor of 2 in the quantum circuit than the third state in Eq. (2.6) due to the $\frac{1}{\sqrt{2}}$ normalization coefficient in $SH\psi$. I account for this in the data collection (Appendix A). Now that all the states are matched to qubits and quantum gates, the operator O_A is matched.

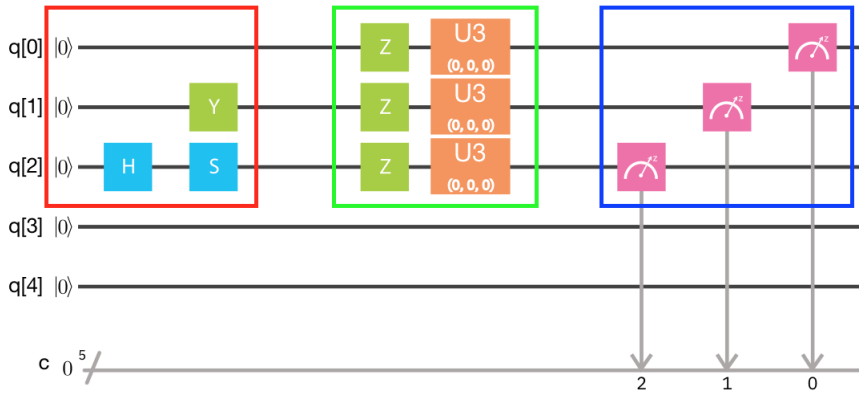

Figure 2.2 EDUR Quantum Circuit for error in Y. The red box encloses the state preparation of the qubits. The green box encloses the O_A operator. The blue box encloses the measurement gates. Note, the U3 gate is evaluated at (0,0,0) in this picture, but is actually evaluated at varying θ and ϕ values.

Using a general gate $U3$ and a Z gate, I implement O_A using $U3Z$. To match the O_A matrix exactly, I evaluate the $U3$ gate at $\lambda = -\phi$, $U3Z$ equals Eq. (2.5).

Now that all the states and operators are matched to combinations of quantum gates and qubits, the gates are implemented as the quantum circuit in Fig. 2.2. The red box shows the first stage—qubit preparation. The green box shows the operator O_A operating on the prepared qubit. The blue box is where the qubits are measured along the z-axis of the Bloch sphere. The same process is repeated for Eq. (1.6) evaluated with $B = X$ and $B = Z$. The resulting quantum circuits for Eqs. (1.5) and (1.6) are shown in Fig. 2.3.

The resulting quantum circuits shown in Figs. 2.2 and 2.3 are evaluated using the QISKit backend for faster data collection and processing (Appendix A) [14]. For all EDURs, ϕ and θ are incremented by $\frac{\pi}{6}$ to see the data fill the allowed value space but not too many data points that the allowed value space is cluttered. To get error and disturbance values over the entire Bloch sphere (including some overlap), θ was varied between

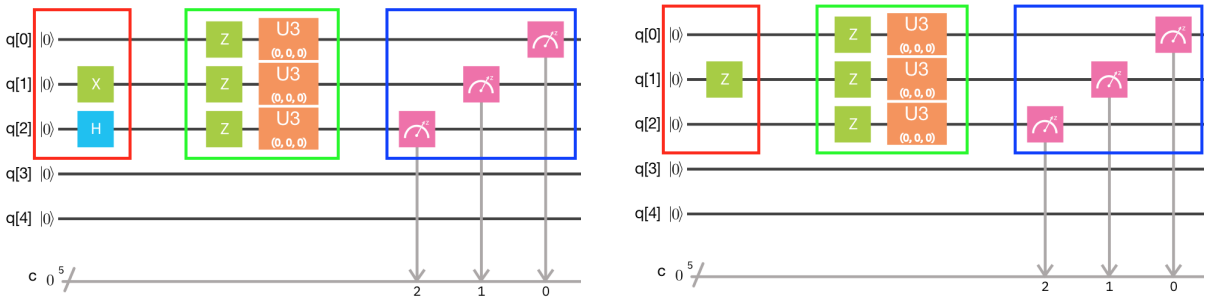

(a) EDUR Quantum Circuit: Disturbance in X

(b) EDUR Quantum Circuit: Disturbance in Z

Figure 2.3 EDUR Quantum Circuit with disturbance in X and Z. For both circuits, the red, green, and blue boxes are the same as described in Fig. 2.2.

0 to $\frac{11\pi}{6}$ and ϕ from 0 to $\frac{11\pi}{6}$. Quantum circuits can be executed multiple times upon one execution request; the number of repeated executions are called shots [13]. I ran each quantum circuit with the maximum number of shots (8192) to ensure the smallest possible standard deviation. Using the quantum computer data, I now compare that data to the two- and three-observable EDUR.

Chapter 3

Results and Conclusion

The main in results of this thesis are found in the three-observable EDUR Eq. (2.2) and the quantum circuits of EDURs in application to spin-$\frac{1}{2}$ Figs. 2.2 and 2.3. The data from the quantum circuits—both two- and three-observable spin-$\frac{1}{2}$ EDURs—are now discussed beginning with two-observable EDURs. I end this chapter with conclusions and future work.

3.1 Verification of Two-observable EDUR in Application to Spin-$\frac{1}{2}$

The quantum computer results for the two-observable EDUR, evaluated with error in Y and disturbance in X, validate the relation (Fig. 3.1). The EDUR forbids values in the blue region and allows values in the white regions. Nearly all of the simulated qubit data [Fig. 3.1a] lie within the allowed region while all the real qubit data [Fig. 3.1b] are within the

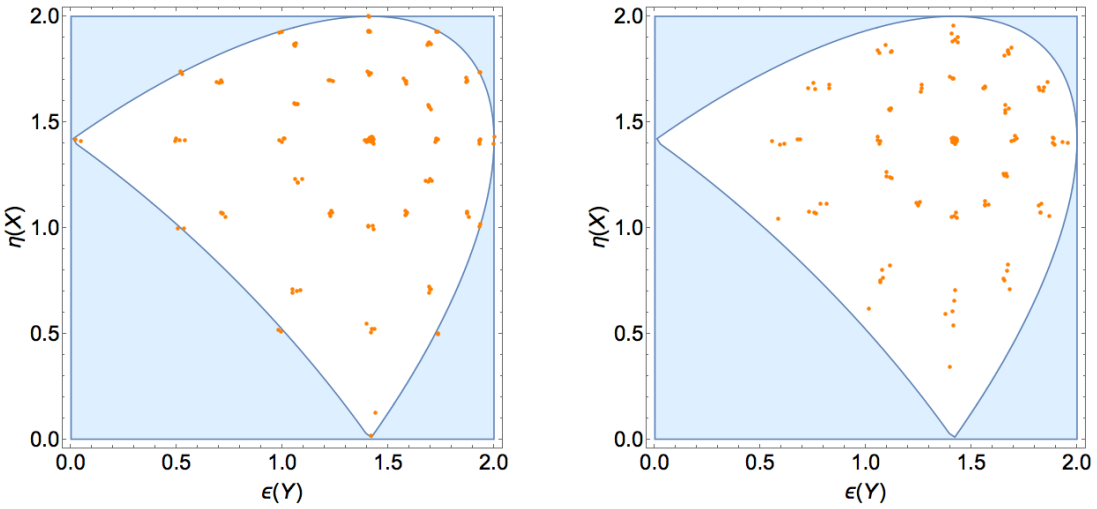

(a) Simulated quantum computer data **(b)** Quantum computer data

Figure 3.1 Two-observable EDUR (error in Y and disturbance in X) with orange data points from simulated (a) and real (b) qubits. Light blue is the forbidden area where the two-observable EDUR would be violated. The orange dots were evaluated in increments of $\frac{\pi}{6}$. Both have a circular like pattern. The larger radii are from larger θ values. By increasing ϕ, a clockwise circle is traced out—starting at the bottom.

allowed region. The outliers in the simulated data are not significantly far enough away from the boundary to be considered violations. The simulated quantum computer uses a random number generator that will, after a large number of samples, center those boundary points on the boundary. The quantum circuits validates the EDUR.

The boundary of the EDUR describes the least amount of error and disturbance tradeoff required. Finding this boundary is the purpose of EDURs. Since the simulated qubits lie along the boundary, the quantum circuits can accurately capture the important physics of EDURs. However, as none of the real qubit data lie on the boundary, the real qubits cannot capture the boundary behavior. Since the simulated data does capture the boundary, but

the real data does not, there are unidentified behaviors within IBM's quantum computers keeping the real qubit data off the boundary.

There is a prominent circle pattern in both sets of data because of the discretized sampling space.

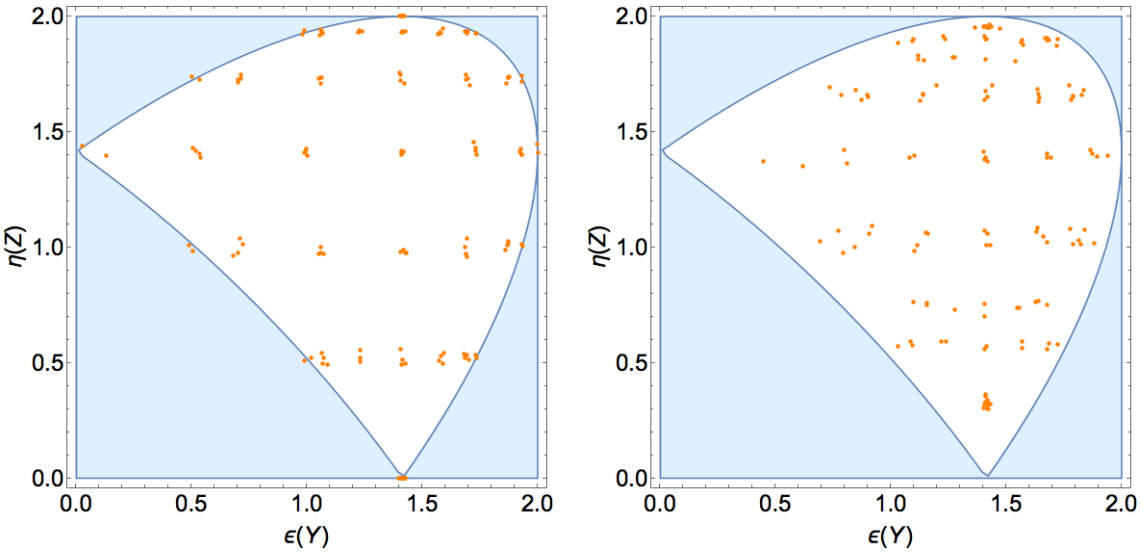

(a) Simulated quantum computer data **(b)** Quantum computer data

Figure 3.2 Two-observable EDUR (error in Y and disturbance in Z) with orange data points from simulated (a) and real (b) qubits. The EDUR forbids values in the light blue region and allows values in the white region. The orange dots were evaluated in increments of $\frac{\pi}{6}$. Both the simulated and qubit data have a horizontal stripe pattern.

I also considered the two-observable EDUR with error in Y and disturbance in Z. The quantum computer results validate this relation as well (Fig. 3.2). The simulated qubit data (in orange) lie within the white allowed region while all the real qubit data are within the allowed region—validating the EDUR. Again, the quantum computer does not capture the boundary. Re-emphasizing my previous conclusion: The quantum computer does not

behave has expected due to some unidentified inner working.

There is a new pattern to the data in Fig. 3.2 compared to Fig. 3.2. The different patterns foreshadow a three dimensional aspect to error and disturbance. Stitched along the error axis into three dimensions, the two two-observable datasets form the three-observable dataset that evaluates the validity of the three-observable EDUR [Eq. (2.4)].

3.2 Verification of Three-observable EDUR in Application to Spin-$\frac{1}{2}$

In the three-observable case, both the simulated and real data do not violate inequality. This supports the validity of the EDUR. The data and the volume have the same diagonal symmetry—another supportive evidence. However, neither the simulated nor the real data come close to the volume-space boundary. To better visualize the volume, I slice it into seven pieces along the $\varepsilon(Y)$-$\eta(X)$ plane. As seen in Figs. 3.3 and 3.4, the light-blue boundary is well past the orange data points for both the simulated and real data. The boundary and data both expand during the first three slices. At $\eta(Z) = 1.00$, the boundary completely disappears. After the fourth slice, the data comes back together, but the theoretical boundary does not. Assuming the data is accurate based on the two-observable EDUR results, then the model needs to be tightened up to the data—specially in those last three slices. A non-tight EDUR is somewhat expected due to half of the equation coming from the general—looser—two-observable EDUR. Overall, the quantum circuits simultaneously show the three-observable EDUR is valid but not tight.

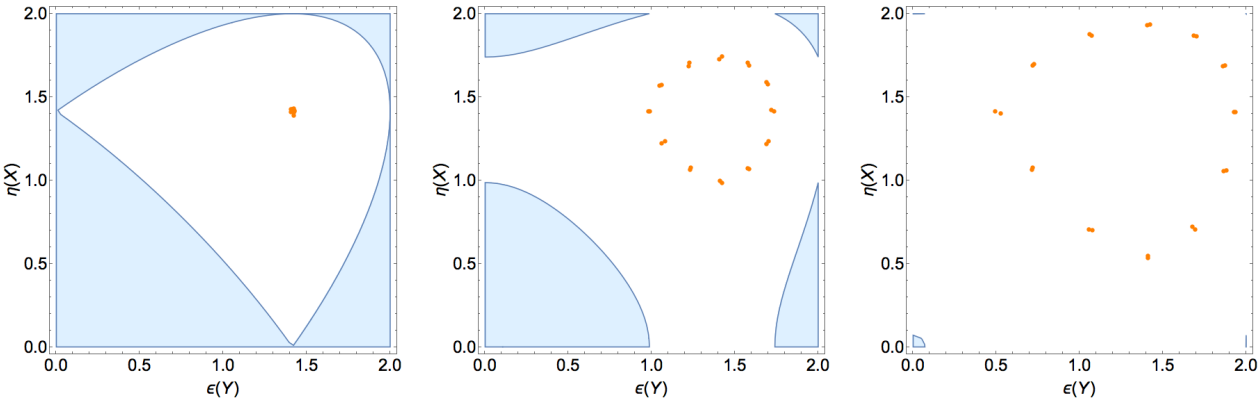

(a) $\eta(Z) = 0.00$ **(b)** $\eta(Z) = 0.51$ **(c)** $\eta(Z) = 0.99$

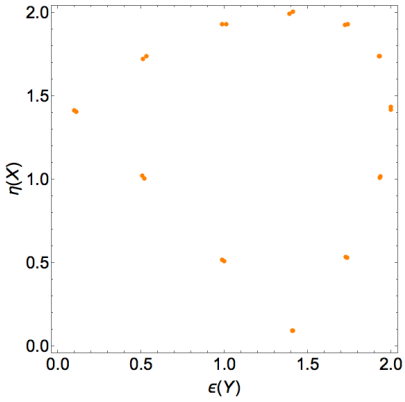

(d) $\eta(Z) = 1.42$

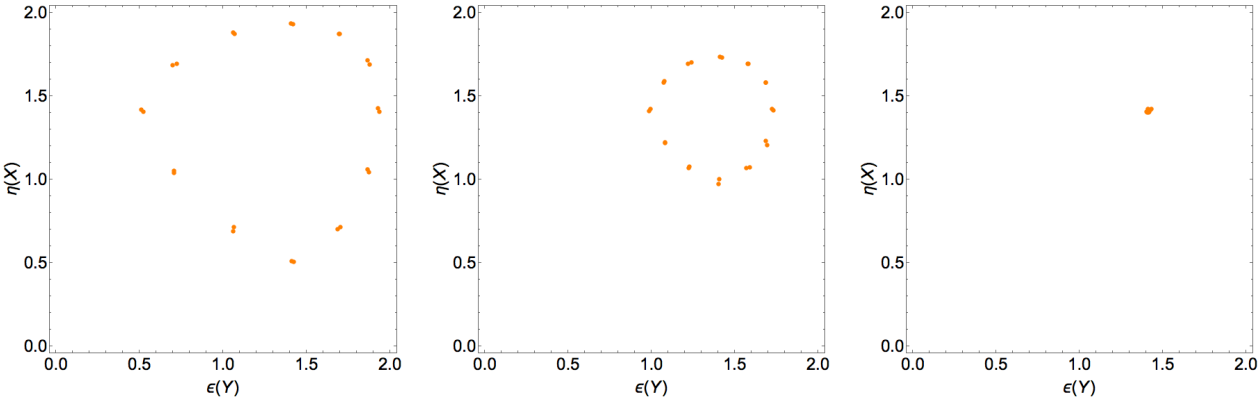

(e) $\eta(Z) = 1.73$ **(f)** 1.93068 **(g)** $\eta(Z) = 2.0$

Figure 3.3 The simulated quantum computer data creates a volume, which I slice into seven pieces along the $\varepsilon(Y)$-$\eta(Z)$ axis. The simulated data is shown as orange dots, while the theoretical allowed area is shown in white. At each slice, the z-component of each cluster of points was averaged with standard deviation < 0.02 for all slices. The mean is displayed in the sub-caption of its plot. As $\eta(Z)$ increases, the forbidden area shrinks to nothing at $\eta(Z) = 1$. The data never meets the boundary. The data even comes back to a single point at $\eta(Z) = 2$ where as the theoretically forbidden area never returns.

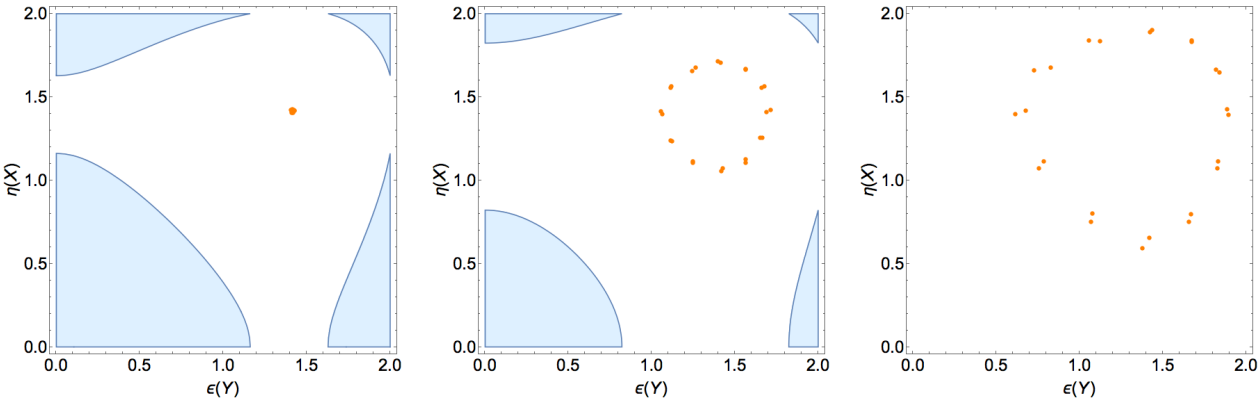

(a) $\eta(Z) = 0.33$ **(b)** $\eta(Z) = 0.66$ **(c)** $\eta(Z) = 1.04$

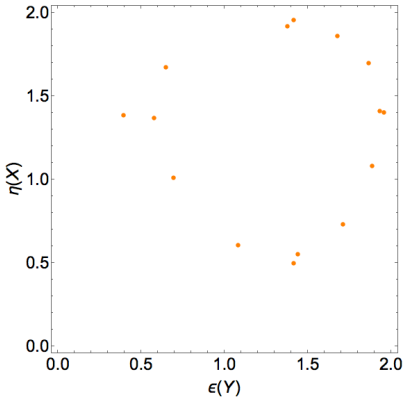

(d) $\eta(Z) = 1.39$

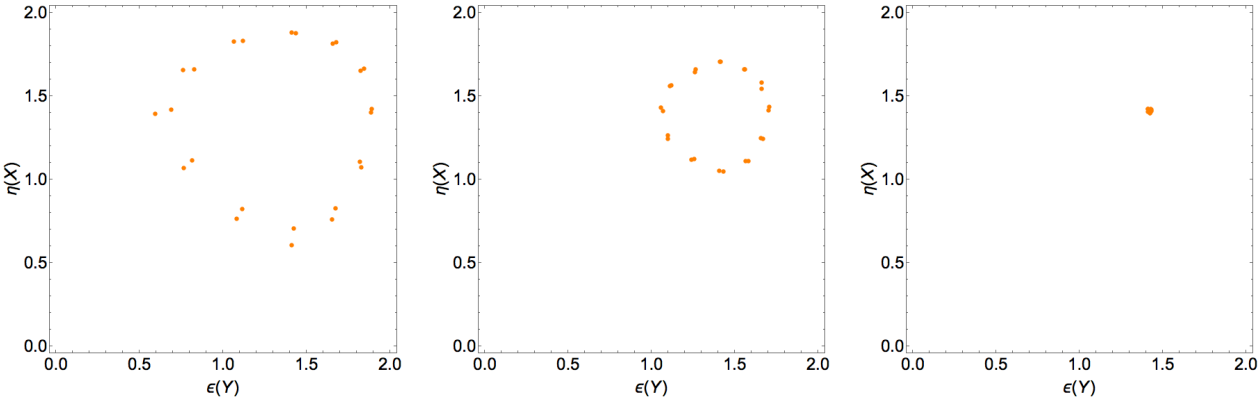

(e) $\eta(Z) = 1.66$ **(f)** $\eta(Z) = 1.87$ **(g)** $\eta(Z) = 1.95$

Figure 3.4 The real quantum computer data creates a volume, which I slice into seven pieces along the $\varepsilon(Y)$-$\eta(Y)$ axis. The data is shown as orange dots, while the theoretical allowed area is shown in white. At each slice, the z-component of each cluster of points was averaged with a standard deviation < 0.088 for all slices. The mean is displayed in the sub-caption of its plot. The fourth subfigure has some missing data points due to gate limitations in the IBM quantum computer. The same growing and shrinking pattern from Fig. 3.3 is seen here. The data never meets the boundary.

3.3 Conclusions

It is possible to consider all possible disturbances from a measurement at once. Not only is such a EDUR derivable [Eqs. 2.2 and 2.4], simulated and real data supported its validity. The context of this validation is important: the EDUR is not tight. The significant spacing between the data and the slices in Figs. 3.4 and Fig. 3.3 shows the need for a tighter three-observable EDUR.

IBM's quantum computer can validate two-observable EDURs, but lacks important boundary validation. Some internal workings are limiting the quantum computer's ability to model the boundary. Though IBM gives calibration data that can be used to reduce some errors, taking calibrations into account does not explain the difference between the boundary and data. Since the data is kept off the lower limit of the EDUR, EDURs may be considered as an error test or characterization method for quantum computers.

Quantum computers, though in their infancy, can model fundamental quantum phenomena. Though this thesis only showed valid modeling to be true for the specific case of EDURs, I believe quantum circuits for many quantum systems can be used to model quantum physics.

3.4 Future Work

The three-observable EDUR needs to be tightened. Though it has a limiting boundary, it appears from the qubit data, that boundary is not low enough. Tightening will bring the theoretical boundary closer to the measured boundary. A more rigorous three-observable EDUR derivation may be required to obtain a tight relation.

Finding the cause for differences between the quantum computer and simulated quantum computer data is another area of future work. Identifying differences may lead to better error characterization in the qubits. For example, there may be specific angles which the U3 gate is less accurate.

I acknowledge use of the IBM Q experience for this work. The views expressed are those of the authors and do not reflect the official policy or position of IBM or the IBM Q experience team.

Appendix A

Quantum Computing Code

This appendix shows the python code used to access IBM's quantum computers and process the data results into error and disturbance terms.

```
import sys
sys.path.append('../../')

#import IBM's quantum computer packages
from qiskit import QuantumProgram
import Qconfig

# useful additional packages
import numpy as np
from scipy.stats import norm, f, t
from scipy.optimize import curve_fit
from pprint import pprint
import csv
import time
import datetime
import math

from IBMQuantumExperience.IBMQuantumExperience import IBMQuantumExperience
```

```
api = IBMQuantumExperience(Qconfig.APItoken, Qconfig.config, True)

#Find error in Y and disturbance in X
#state prepared in Z
qp = QuantumProgram()
qp.set_api(Qconfig.APItoken, Qconfig.config['url']) # set the APIToken and API url

n = 5 #number of qubits initiated (only one is used though)
i = 3 #select qubit with least error

q = qp.create_quantum_register('q',n)
c = qp.create_classical_register('c',n)
#for simulated data use:
#backend = 'local_qasm_simulator'
backend = 'ibmqx2'

circuits = ['EOa','EAOa','Elots','DOb','DBOb','Dlots']
increment = math.pi/6
shots = 8192

theta = 0
while theta < 2*math.pi:
    phi = 0
    while phi < 2*math.pi:
        # quantum circuit for error in Y
        EOa = qp.create_circuit('EOa',[q],[c])
        EAOa = qp.create_circuit('EAOa',[q],[c])
        Elots = qp.create_circuit('Elots',[q],[c])
        EOa.z(q[i])
        EOa.u3(theta,phi,-phi,q[i])
        EOa.measure(q[i],c[0])
        EAOa.y(q[i])
        EAOa.z(q[i])
        EAOa.u3(theta,phi,-phi,q[i])
        EAOa.measure(q[i],c[0])
```

```
Elots.h(q[i])
Elots.s(q[i])
Elots.z(q[i])
Elots.u3(theta,phi,-phi,q[i])
Elots.measure(q[i],c[0])

# quantum circuit for distrubance in X
DOb = qp.create_circuit('DOb',[q],[c])
DBOb = qp.create_circuit('DBOb',[q],[c])
Dlots = qp.create_circuit('Dlots',[q],[c])
DOb.z(q[i])
DOb.u3(theta,phi,-phi,q[i])
DOb.measure(q[i],c[0])
DBOb.x(q[i])
DBOb.z(q[i])
DBOb.u3(theta,phi,-phi,q[i])
DBOb.measure(q[i],c[0])
Dlots.h(q[i])
Dlots.z(q[i])
Dlots.u3(theta,phi,-phi,q[i])
Dlots.measure(q[i],c[0])

# Execute the quantum circuit
result = qp.execute(circuits, backend, shots=shots, max_credits=5, wait=20, timeout=7000)

EOa,EAOa,E3rd,DOb,DBOb,D3rd = 0,0,0,0,0,0

EOa = float(marginal_counts(result.get_counts('EOa'), [i])['0'])/shots
EOa -= float(marginal_counts(result.get_counts('EOa'), [i])['1'])/shots
EAOa = float(marginal_counts(result.get_counts('EAOa'), [i])['0'])/shots
EAOa -= float(marginal_counts(result.get_counts('EAOa'), [i])['1'])/shots
E3rd = float(marginal_counts(result.get_counts('Elots'), [i])['0'])/shots
E3rd -= float(marginal_counts(result.get_counts('Elots'), [i])['1'])/shots
DOb = float(marginal_counts(result.get_counts('DOb'), [i])['0'])/shots
DOb -= float(marginal_counts(result.get_counts('DOb'), [i])['1'])/shots
```

```
        DBOb = float(marginal_counts(result.get_counts('DBOb'), [i])['0'])/shots
        DBOb -= float(marginal_counts(result.get_counts('DBOb'), [i])['1'])/shots
        D3rd = float(marginal_counts(result.get_counts('Dlots'), [i])['0'])/shots
        D3rd -= float(marginal_counts(result.get_counts('Dlots'), [i])['1'])/shots

        error = math.sqrt(math.fabs(2+EOa+EAOa-2*E3rd))
        dist = math.sqrt(math.fabs(2+DOb+DBOb-2*D3rd))

        #increment phi and count
        phi += increment
    theta += increment


#state prepared in z
#finds error in y and disturbance in z
qp2 = QuantumProgram()
qp2.set_api(Qconfig.APItoken, Qconfig.config['url']) # set the APIToken and API url

q = qp2.create_quantum_register('q',n)
c = qp2.create_classical_register('c',n)

theta = 0
while theta <= 2*math.pi:
    phi = 0
    while phi < 2*math.pi:
        # quantum circuit for error in Y
        EOa = qp2.create_circuit('EOa',[q],[c])
        EAOa = qp2.create_circuit('EAOa',[q],[c])
        Elots = qp2.create_circuit('Elots',[q],[c])
        EOa.z(q[i])
        EOa.u3(theta,phi,-phi,q[i])
        EOa.measure(q[i],c[0])
        EAOa.y(q[i])
        EAOa.z(q[i])
        EAOa.u3(theta,phi,-phi,q[i])
```

```
EAOa.measure(q[i],c[0])
Elots.h(q[i])
Elots.s(q[i])
Elots.z(q[i])
Elots.u3(theta,phi,-phi,q[i])
Elots.measure(q[i],c[0])

# quantum circuit for distrubance in Z
DOb = qp2.create_circuit('DOb',[q],[c])
DBOb = qp2.create_circuit('DBOb',[q],[c])
Dlots = qp2.create_circuit('Dlots',[q],[c])
DOb.z(q[i])
DOb.u3(theta,phi,-phi,q[i])
DOb.measure(q[i],c[0])
DBOb.z(q[i])
DBOb.z(q[i])
DBOb.u3(theta,phi,-phi,q[i])
DBOb.measure(q[i],c[0])
Dlots.z(q[i])
Dlots.u3(theta,phi,-phi,q[i])
Dlots.measure(q[i],c[0])

# Execute the quantum circuit
result = qp2.execute(circuits, backend, shots=shots, max_credits=5, wait=20, timeout=7000)

EOa,EAOa,E3rd,DOb,DBOb,D3rd = 0,0,0,0,0,0

EOa = float(marginal_counts(result.get_counts('EOa'), [i])['0'])/shots
EOa -= float(marginal_counts(result.get_counts('EOa'), [i])['1'])/shots
EAOa = float(marginal_counts(result.get_counts('EAOa'), [i])['0'])/shots
EAOa -= float(marginal_counts(result.get_counts('EAOa'), [i])['1'])/shots
E3rd = float(marginal_counts(result.get_counts('Elots'), [i])['0'])/shots
E3rd -= float(marginal_counts(result.get_counts('Elots'), [i])['1'])/shots
DOb = float(marginal_counts(result.get_counts('DOb'), [i])['0'])/shots
DOb -= float(marginal_counts(result.get_counts('DOb'), [i])['1'])/shots
```

```
        DBOb = float(marginal_counts(result.get_counts('DBOb'), [i])['0'])/shots
        DBOb -= float(marginal_counts(result.get_counts('DBOb'), [i])['1'])/shots
        D3rd = float(marginal_counts(result.get_counts('Dlots'), [i])['0'])/shots
        D3rd -= float(marginal_counts(result.get_counts('Dlots'), [i])['1'])/shots

        error = math.sqrt(math.fabs(2+EOa+EAOa-2*E3rd))
        dist = math.sqrt(math.fabs(2+DOb+DBOb-2*D3rd))

        #increment phi and count
        phi += increment
    theta += increment
```

Bibliography

[1] W. Heisenberg, "The Physical Content of Quantum Kinematics and Mechanics," In: Wheeler, J.A. and Zurek, W.H., Eds., Quantum Theory and Measurement, Princeton University Press, Princeton, 62-84. [Originally Published: Z. Phys., 1927, 43(3-4), 172-198] (1927).

[2] M. Ozawa, "Universally valid reformulation of the Heisenberg uncertainty principle on noise and disturbance in measurement," Phys. Rev. A **67,** 042105 (2003).

[3] M. Ozawa, "Physical content of Heisenberg's uncertainty relation: Limitation and reformulation," Phys. Lett. A **318,** 21–29 (2003).

[4] M. Ozawa, "Uncertainty relations for joint measurements of noncommuting observables," Phys. Lett. A **320,** 367–374 (2004).

[5] M. Ozawa, "Uncertainty relations for noise and disturbance in generalized quantum measurements," Annals of Physics **311,** 350–416 (2004).

[6] J. Collings, "Quantifying the Uncertainty of the Heisenberg Uncertainty Relation: Preparation vs. Measurement Uncertainty," BYU Senior Thesis (2015).

[7] C. Branciard, "Error-tradeoff and error-disturbance relations for incompatible quantum measurements," Proc. Natl. Acad. Sci. **110,** 6742–6747 (2013).

[8] M. Ozawa, "Error-disturbance relations in mixed states," arXiv:1404.3388v1 [quant-ph] (2014).

[9] G. Sulyok *et al.*, "Violation of Heisenberg's error-disturbance uncertainty relation in neutron-spin measurements," Phys. Rev. A **88,** 022110 (2013).

[10] B. Demirel *et al.*, "Experimental Test of Residual Error-Disturbance Uncertainty Relations for Mixed Spin-1/2 States," Phys. Rev. Lett. **117,** 140402 (2016).

[11] B. Demirel *et al.*, "Experimental test of an entropic measurement uncertainty relation for arbitrary qubit observables," arXiv:1711.05023v1 [quant-ph] (2017).

[12] M. Ringbauer *et al.*, "Experimental Joint Quantum Measurements with Minimum Uncertainty," Phys. Rev. Lett. **112,** 020401 (2014).

[13] L. Bishop, A. Corcoles, A. Cross, A. Cross, and J. Gambetta, "Full User's Guide," https://quantumexperience.ng.bluemix.net/qx/tutorial?sectionId=full-user-guide&page=introduction (2018).

[14] IBM Research *et al.*, "QISKit Website," https://www.qiskit.org (2018).

[15] H. Robertson, "The Uncertainty Principle," Phys. Rev. **34,** 163 (1929).

[16] W. Ma *et al.*, "Experimental Demonstration of Uncertainty Relations for the Triple Components of Angular Momentum," Phys. Rev. Lett. **118,** 180402 (2017).

[17] H. Qin, S. Fei, and G. X. Li-Jost, "Multi-observable Uncertainty Relations in Product Form of Variances," Sci. Rep. **6,** 31192 (2016).

Index

Bloch sphere, 14

Disturbance
    definition of, 3
    measurement equation of, 5
    quantum circuit, 18

Error
    definition of, 2
    measurement equation of, 5
    quantum circuit, 17

IBM Q Experience, 5
    Composer page, 6
    QISKit, 17
    QISKit code, 27

Three-observable EDUR
    general equation, 11
    real quantum computer data plot, 24
    simulated quantum computer data plot, 23
    tighter equation, 12
Two-observable EDUR
    general equation, 4
    quantum computer data $Y - X$ plot, 20
    quantum computer data $Y - Z$ plot, 21
    tighter equation, 4